Effect of NH₃ Concentration on the Performance of Nitrogen doped TiO₂ Photoelectrochemical Cell

Akrajas Ali Umar[1,], Mohd Yusri Abd Rahman[2,*], Siti Khatijah Md Saad[2], Muhamad Mat Salleh[1]*

[1] Institute of Microengineering and Nanoelectronics, Universiti Kebangsaan Malaysia, 43600 UKM Bangi, Selangor, Malaysia
[2] College of Engineering, Universiti Tenaga Nasional, Km 7, Jalan Kajang-Puchong, 43009 Kajang, Selangor, Malaysia
[*]E-mail: akrajas@ukm.my, yusri@uniten.edu.my

TiO₂ nanostructures film synthesized using liquid phase deposition method (LPD) was used as photovoltaic material in photoelectrochemical cell. The anatase phase of TiO₂ nanostructures was obtained by annealing the TiO₂ samples at a temperature of 400 ^{o}C before undergoing NH₃ treatment with various concentrations, namely, 2.5, 5.0, 7.5, 10.0 and 12.5%. X-ray diffraction (XRD), field emission scanning electron microscope (FESEM), fourier transform infrared (FT-IR) and UV-Vis spectroscopy were performed to characterize the samples. The anatase phase of the TiO₂ film was about 240 nm in thickness and 20 nm in diameter with the measured band gap ranging from 2.97 to 3.1 eV for the treated samples. The highest J_{sc} and power conversion efficiency were 0.76 mA cm^{-2} and 0.14% obtained from the cell fabricated with 7.5 % NH₃.

1. INTRODUCTION

TiO₂ nanoparticles have widely been utilized as photovoltaic material in photoelectrochemical and photocatalytic due to its wide band gap and high refractive index [1]. In photoelectrochemical cell, photoexcitation occured in semiconductor material that absorbs sunlight in order to generate photocurrent. For the photoexcitation to occur, the absorption of light in longer wavelength region is needed as TiO₂ have large band gap energy of 3.2 eV [2]. However, TiO₂ has low absorption coefficient in the visible region and near infrared region which had caused only small fraction of sunlight to be absorbed [1]. Thus, the photocurrent generation from the sunlight is not effective as the

solar spectrum lay in the visible region. Hence, it is important to modify the photoresponse of TiO_2 so that the light absorption of TiO_2 can cover the visible region. Thus, producing TiO_2 nanoparticle with higher photoresponse are highly demanded. In photoelectrochemical cell, the excitation of electrons from TiO_2 valence band towards conduction band leaves them with deficit in electrons. This oxidized TiO_2 will be reduced back to its original state by accepting electrons from triiodide of electrolyte. The triiodide will be recovering their electrons by completing their migration towards counter electrode [3]. The migration of the electrons results in photocurrent and the efficiency of the photon to photocurrent conversion can be determined. For the electrons to be excited, it is important to lower the band gap of TiO_2 so that lesser energy required for an electron to jump from valence band towards conduction band [4]. It is well known that the TiO_2 itself has high energy band gap of 3.2 eV, making electrons jump difficult to occur. The photoresponse of TiO_2 can be enhanced by extending the absorption windows of TiO_2 from UV to visible region and lowering the band gap energy of TiO_2 nanomaterial. Several successful methods have been reported in extending the absorption windows for the TiO_2 nanomaterial such non-metal doping, metal doping and plasma treatment [1, 5-6]. Even though these methods provide a satisfying result, however they are not as effective as the producing cost were higher and difficult to prepare.

The enhancement of the photoresponse of TiO_2 by introducing non-metal dopants in the nanomaterials with common dopants used such as N, F, O and S were widely studied as it is more effective compared to other methods. The dopants used in photoelectrochemical cell have found to provide much broader optical absorption windows and contributes to the band gap narrowing [7]. However, nitrogen as dopant was commonly used in photoelectrochemical cell as the nitrogen doping preparation was found to be simpler. It was also found that the nitridization of the TiO_2 nanoparticles help to enlarge the absorption spectrum window of UV light [5]. Several methods have been proposed in producing the nitrogen doping TiO_2 thin film nanoparticles such as solvolthermal [8], sol-gel [9], spray pyrolysis [10], hydrothermal [11], anodization [12] and sputtering technique [13]. Few structures such as nanothorn [8], nanorice grain [9], nanoplate [10], nanotubes [11], nanoflower [12] and nanosheet [14] were either used or produced in studying the nitrogen doping on TiO_2 as these structures possessed large surface area in which has proven to increase the efficiency of the photoelectrochemical cell and photocatalyts.

In this paper, we discuss the performance of photoelectrochemical cell utilizing TiO_2 thin film treated with NH_3 water as the photovoltaic material. We have successfully performed the nitrogen doping on the TiO_2 nanoparticles by modifying the concentration of the NH_3 water. The TiO_2 nanoparticles were firstly synthesized via liquid phase deposition (LPD) techniques where nanograss structure was obtained. Liquid phase deposition method is a method which involved formation of metal oxide thin film with the hydrolysis of metal-flouro cations [15]. This method requires only the immersion of the ITO substrate in a mixed solution of the titanate-flouro cations as the source and boric acid as flouride scavenger simultaneously [16]. The samples TiO_2 were then used as photovoltaic material for photoelectrochemical cell of ITO/TiO_2/liquid electrolyte/Platinum. From the study, we found that the incorporation of ammonium as nitrogen dopant source in TiO_2 helped to enlarge the absorption windows of the TiO_2 nanoparticles, thus improving the performance of the cell. This is due

the band gap of the N-doped TiO_2 was found to be slightly decreased from the undoped TiO_2 sample which is 3.2 eV.

2. EXPERIMENTAL PROCEDURE

2.1 Materials

Ammonium hexaflourotitanate $(NH_4)_2TiF_6$ and boric acid were purchased from Sigma-Aldrich and Wako Chemical, respectively. The NH_3 used for the treatment study was ammonium hydroxide of 30% in water. ITO-coated glass was purchased from VinKarola instrument USA with the sheet resistance of 9-22 Ω per square.

2.2 Synthesis of TiO₂ nanoparticle

TiO_2 nanostructures were prepared using LPD method. ITO substrates underwent standard cleaning procedure where they were cleaned using acetone and ethanol in sequence. The cleaned substrates were dipped in the growth solution of 5 ml 0.1 M $(NH_4)_2TiF_6$ and 5 ml 0.2 M H_3BO_3 vertically for 25 hours with two growth times [16]. The growth process was carried out under room temperature. The as prepared nanostructured TiO_2 was rinsed and dried before it was annealed at 400 ^{o}C for 30 minutes. Growth of the TiO_2 nanoparticles was started with hydrolysis of the metal flouro cation used $((NH_4)_2TiF_6)$ with boric acid was used to scavenge the flouro cation left. TiO_2 nanoparticles film formed on the surface was then subjected towards annealing process to purify the metal oxide nanoparticles produce and to remove organic materials left during the hydrolysis process. The NH_3 treatment with various percentage of 0.6 mL NH_3 in water solution, namely, 2.5, 5, 7.5, 10, and 12.5% were performed onto the TiO_2 samples using spin-coating technique for 30 s. The treated samples were then subjected towards heating at 100 ^{o}C for 15 minutes to remove any hydroxyl compounds.

2.3 TiO₂ nanoparticle characterization

The surface morphology of untreated and treated NH_3 TiO_2 nanostructures were observed using field emission scanning electron microscope (FESEM) technique (ZEiSS SUPRA 55 VP. The crystallinity of the untreated and treated TiO_2 were studied using X-ray diffraction method (BRUKER D8 Advance) with the diffraction angle of 0-60° using Cu Kα radiation (λ = 0.154 nm). The optical properties of the untreated and treated samples were investigated by obtaining the absorption spectra of the samples using UV-VIS spectrophotometer (Lambda 900 PERKIN ELMER) in the wavelength range of 350 to 900 nm. Fourier transform infrared was used to determine the molecular and lattice vibrations of the samples using PERKIN ELMER SPECTRUM 400 FT-IR/FT-NIR in the wavenumber range of 650 to 4000 cm^{-1}. The investigation of the interfacial molecule binding of NH_3 and TiO_2 surface was also performed by FTIR characterization.

2.4 Photoelectrochemical fabrication and performance study

The treated and untreated photovoltaic material was separately sandwiched together with a platinum counter electrode. The electrode was prepared by sputtering the platinum source for 4 minutes on bare ITO glass. The electrolyte consists of 0.5 M tetrabutylammoniun iodide, 0.05 M I2 and 0. 5 M 4-tertbutylpyridine in acetonitrile was then injected through the space between TiO_2 layer and platinum counter electrode. The current-voltage measurements of the cells were performed using a Keithley model 237 under simulated AM 1.5 light source illumination of 100 m Wcm^{-2}.

3. RESULTS AND DISCUSSION

3.1 Surface morphology

Figure 1 shows the surface morphology of the synthesized TiO_2 nanostructures for the (a) untreated and treated TiO_2 nanostructures with various concentrations at the magnification of 50000×. It was found from the FESEM micrographs that the TiO_2 nanoparticles were uniform even though the hydrolysis process took 25 hours despite has been reported before that agglomeration of nanoparticles would occur if the hydrolysis process took too long [17].
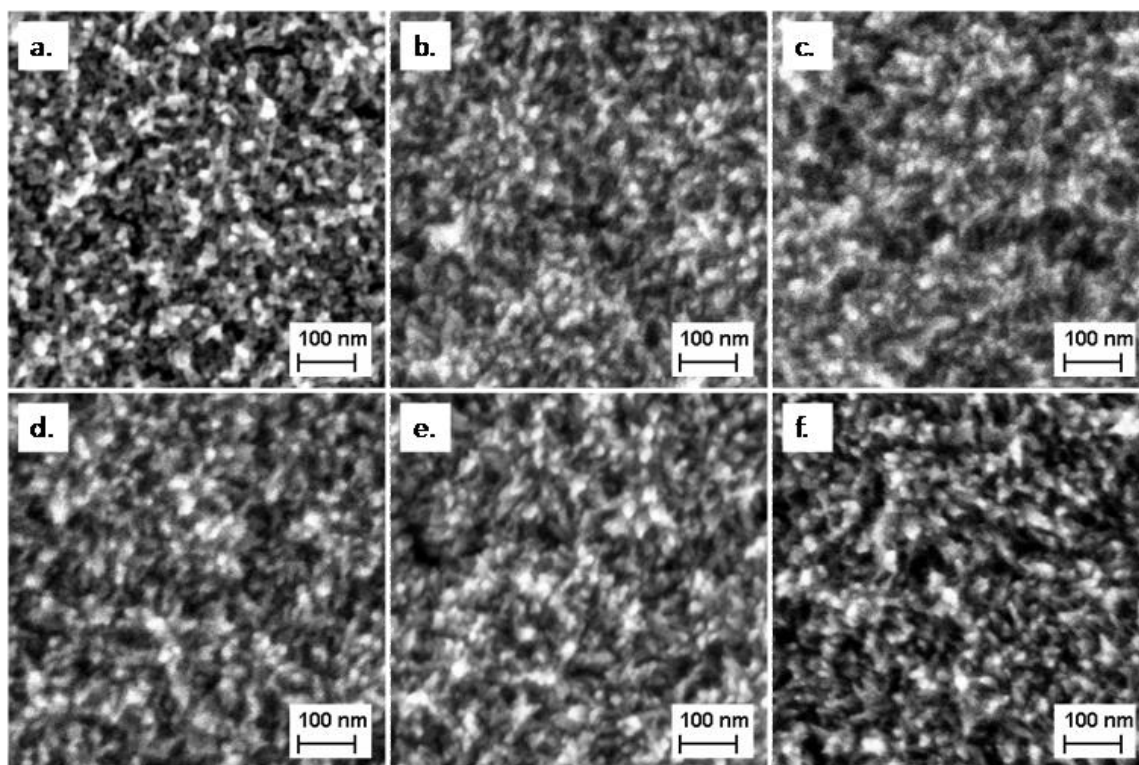

Figure 1. Surface morphology of (a) untreated and treated TiO_2 nanostructures with (b) 2.5, (c) 5.0, (d) 7.5, (e) 10 and (f) 12.5 % NH_3 with the magnification of 50000×

This may be due to the fine surface of our substrate and the substrate itself was hung vertically compared to the reported substrate. The nanostructures for both treated and untreated TiO_2 showed a pack vertical nanograss-like morphology. From Figure 1, the arm-length of each individual nanoparticles was found to be ~20 nm and the arm length remains the same even with the samples treated with NH_3 with different concentration. The thickness for untreated and treated samples was found to be ~240 nm.

The structures remains the same for all the NH_3 treated TiO_2 even though the cracks were visible due to the surface tension arises from the growth process and the annealing temperature performed on the samples as the non-annealed sample was found to be crack-free. This visibly unchanged morphology of the TiO_2 nanostructures can be explained by the low concentration of the dopants and the substitution of the N species only occurs at the surface of the anatase plane of TiO_2. The nanoparticle growth exhibits a highly dense nanoparticles growth should have provided a large surface area. It is important for the grown nanoparticles to be high in surface area as for the electrons jump upon light illumination and for the electrons transfer to take place in redox couples reaction. The thickness of the synthesized nanoparticles should also be thick enough to prevent the recombination process to take place.

3.2 X-Ray diffraction

Figure 2 shows the XRD spectra of the untreated and treated TiO_2 nanostructures annealed at 400 ^{o}C. All the peaks observed match the JCPDS of anatase phase of TiO_2 (File no 21-1272) where the peaks related to (101), (004), (200) and (211) corresponding with the diffraction angles of 24.8, 37.5, 48 and 54.2^o, respectively. Unfortunately, from the spectra there is no clear distinguishing between the treated and untreated samples as the N incorporated for the treated samples was very low in concentration and it is expected that the incorporation of the NH_3 molecules would only occur at the surface of the TiO_2 nanoparticles. It can be understood that the TiO_2 nanostructures growth orientation is towards the 101 direction as the presence of the strong peak related to the crystalline phase. The orientation peak for 101 plane for the treated samples were found to be shifted towards the larger angle matching with the previously reported work [17].

However, the peak shift was very small in angle as it only can be determined only by using EVA software provided. From the spectra analysis, we can assumed that the ions infusion of the NH_3 used as the nitrogen source had caused a distortion in the lattice resulting in deflecting of the x-ray beam towards larger angle and it is expected that the adsorption of NH_3 species was more favorable or done by titanium atoms instead of oxygen atoms at the surface of the anatase phase of 101 plane.

The crystallite size and the lattice parameter for the tetragonal system of anatase TiO_2 determined by Debye-Scherrer equation and the TOPAS software are listed in Table 1. From the table, the clear trend of the variation of the crystallite size and lattice parameter of treated TiO_2 nanoparticles with the concentration of NH_3 are not seen. However, the largest crystallite size is observed at 7.5% sample. This shows that nanoparticles grain growth was enhanced through NH_3 treatment.
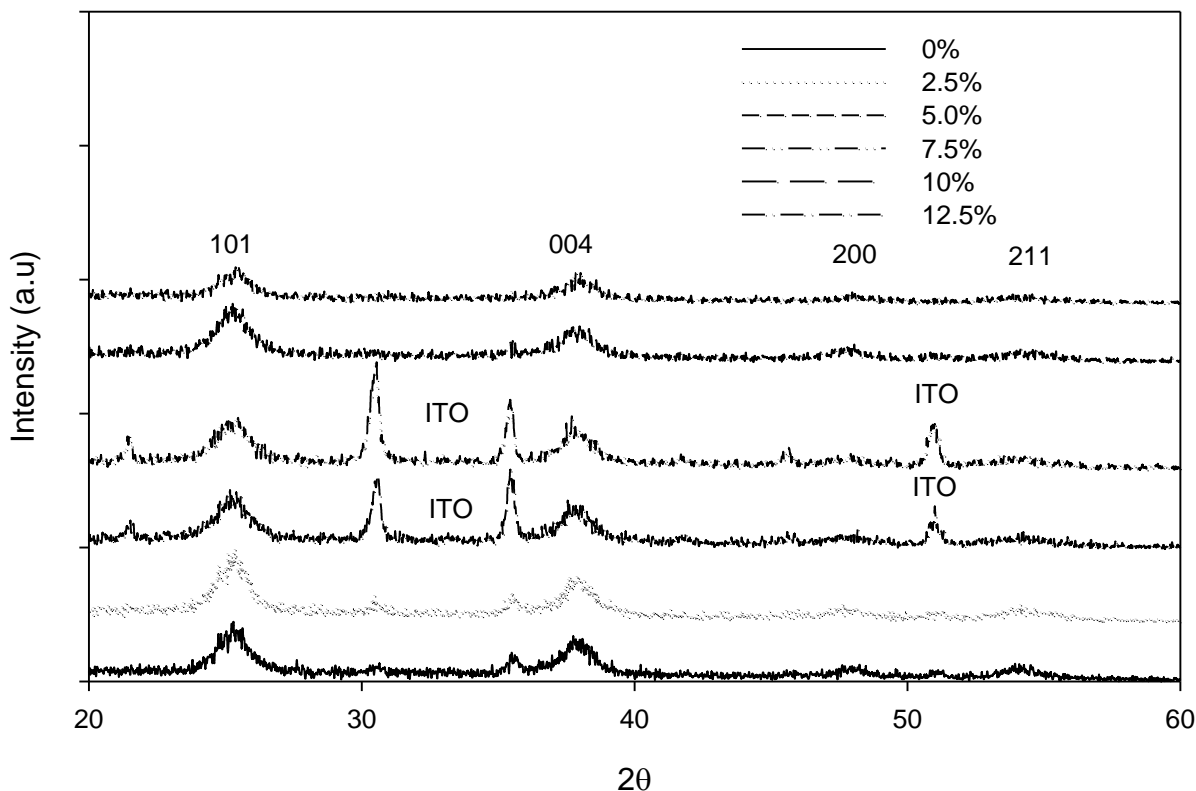
Figure 2. X-ray diffraction spectra of untreated and treated TiO_2 nanostructures with various concentrations of NH_3

Table 1. Crystallite size and lattice parameter value for TiO_2 treated with various NH_3 concentrations

Sample	Crystallite Size (nm)	Lattice Parameter (Å)	
(% NH3)		a	c
0	14.1	3.781	9.456
2.5	18.6	3.792	9.503
5.0	15.5	3.785	9.497
7.5	22.6	3.788	9.497
10.0	18.0	3.793	9.508
12.5	15.7	3.787	9.498

3.3 Fourier Transform Infra Red Spectra

Figure 3 shows the FTIR spectra of the untreated and the treated TiO_2 with various percentage of NH_3 concentrations. FTIR characterization also shows the possible presence of nitrogen ions in the anatase TiO_2 samples prepared. All the treated NH_3 TiO_2 samples exhibits a bands at 3160-3280, 1880-1960, 1630-1640, and 1240 cm^{-1}. The broad and strong band at the 3160-3280 cm^{-1} was attributed by the molecular stretching of NH_3 itself [18]. The broad band ranging from 1880-1960 cm^{-1} shows the stretching of N-N complexes indicating that the presence of the N species exists in the treated samples

[19]. The bending of the ammonium cations presence also can be observed by the weak band which appears at 1650 cm^{-1} [20]. These two compounds existence shows that the ions infusion from the NH$_3$ as nitrogen source for the TiO$_2$ samples was successful by using this technique. The presence of nitrogen compound in our samples can be confirmed by the dinitrogen anions band. The anatase TiO$_2$ peak for all the samples can be observed by the strong and sharp band at 600 cm^{-1}, represents lattice vibration of the TiO$_2$ nanoparticles used in this works [18].

Generally, the transmittance of the molecule vibrations decreases as the percentage of the NH$_3$ concentration increases as shown in the figure below but the lattice vibration of the TiO$_2$ samples remains the same as the TiO$_2$ sample for both treated and untreated were prepared under the same condition. At 1650 cm^{-1}, the NH$_3$ bending seems to have been shifted towards lower frequency when the percentage of concentration of the NH$_3$ increases showing the weakening of the NH$_3$ bending formed. This weakening bond might has been caused by the formation of the metal-amine complex (Ti-N) [21]. The presence of the ammonium ions in the spectra plotted shows that we have successfully introduced an N species in the TiO$_2$ lattice.
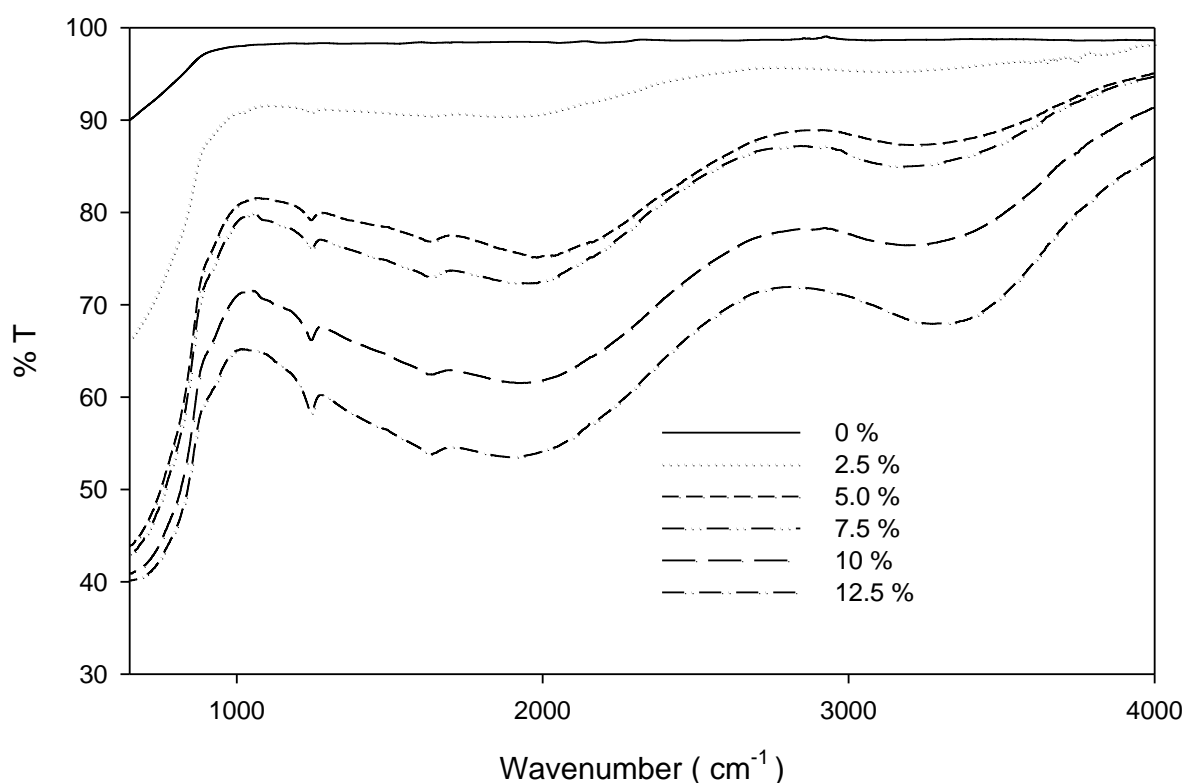

Figure 3. FT-IR spectra for untreated and treated TiO$_2$ nanostructures with various concentrations of NH$_3$

3.4 UV-VIS Absorption Spectra

Figure 4 shows the UV-VIS absorption spectra for untreated and NH$_3$ treated TiO$_2$. All the samples show an absorbance peak at the blue region (400 nm). We can see that the absorption windows for the treated samples were much wider. This is might have been due to the incorporation of

the N dopant source in the TiO_2 lattice. The NH_3 treated TiO_2 samples has introduced an absorption window at 550 nm wavelength region for all the treated TiO_2 samples. The appearance of these new absorption windows was found to be resulting from the excitation of electrons from the occupied state towards the conduction state at this region [9]. The highest absorption obtained for the green region was found to be the TiO_2 samples with the 5.0 % NH_3.

The band gap estimation for all the treated and untreated samples were performed in this region by obtaining the interception of the plotted spectra of *(αhv)$^{1/2}$* versus E_g. The calculated E_g represents the minimum energy needs to be acquired by an electron to jump from the valence band to the conduction band. The E_g for the untreated sample is 3.18 eV and for the treated sample was found to be from in the range of 2.72 to 3.08 eV. The treated TiO_2 samples have lower E_g compared to the untreated TiO_2 sample. The treated TiO_2 samples have much lower E_g was due to the effect of nitrogen species that have been introduced in the TiO_2 lattices resulting in the oxygen vacancies. The introduction of impurities as mentioned above contribute to the narrow band gap of the electronic structure and increases the optical absorption of the treated TiO_2 samples [22].
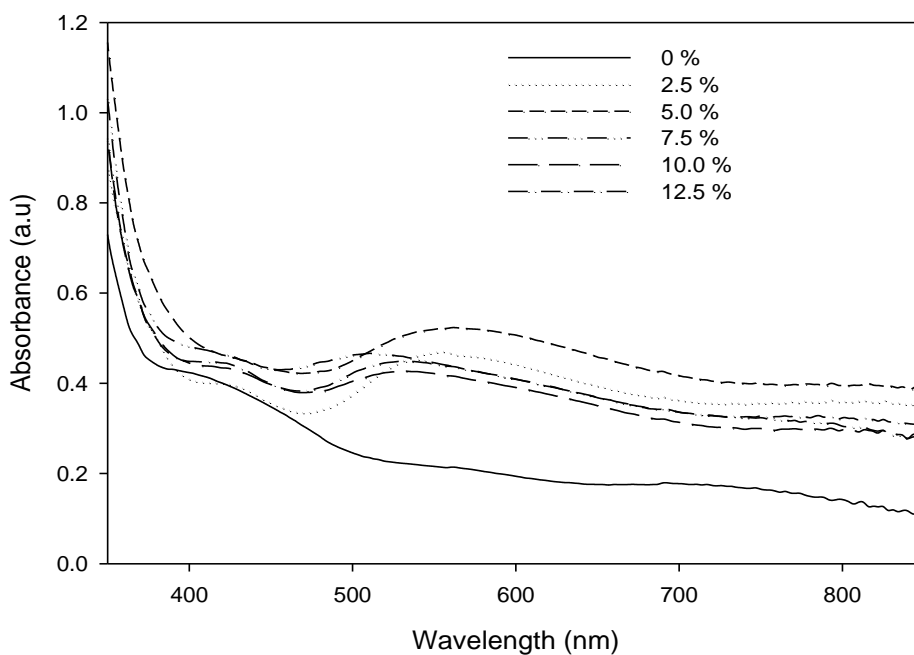

Figure 4. UV-VIS spectra for untreated and treated TiO_2 nanostructures with various concentrations of NH_3

3.5 Photoelectrochemical cell performance

Figure 5 shows the *J-V* curves of the cells utilizing the untreated and treated TiO_2 samples with 2.5, 5.0, 7.5, 10 and 12.5 % NH_3. Table 2 illustrates the photovoltaic parameters of the cells analyzed from Figure 5. From the table, the highest J_{sc} was for TiO_2 sample treated with 7.5 % NH_3 concentration with the value of 0.76 mA cm^{-2}. The open circuit voltage was found to be around 0.36 to

0.48 V. Also, the highest power conversion efficiency of 0.14% was obtained from the cell with the sample treated with the 7.5 % NH_3 concentration. The highest J_{sc} normally leads to the higher efficiency. From the table, we can see that in overall, the samples treated with NH_3 as photovoltaics materials demonstrated much higher efficiency compared to the untreated sample. This might due to the contribution to the optical absorption capability of the NH_3 treated samples as illustared in Figure 4. The 7.5 % NH_3 concentration shows the highest current obtained from the photoelectrochemical cell fabricated might have been due to the fact of the most successful nitridization of the TiO_2 nanoparticles helps to increase the photon yield for light to current conversion. For the samples treated below this concentration, the lower concentrations were not significant enough to exhibit any changes in current obtained in the cells. The nitrogen replacement in the lattice which was explained earlier must have been small enough or they might be no nitrogen replacement at all and the un-replaced nitrogen might have cause hindrance in the samples instead of assisting in the photon yield. The efficiency of the treated cells was then decreased at much higher concentration. This might be due to the fact that the TiO_2 nanoparticles tend to dissolve in concentrated alkalized ambient thus might have lowered the number of photon yield from the light illuminated reducing the light to current conversion efficiency.
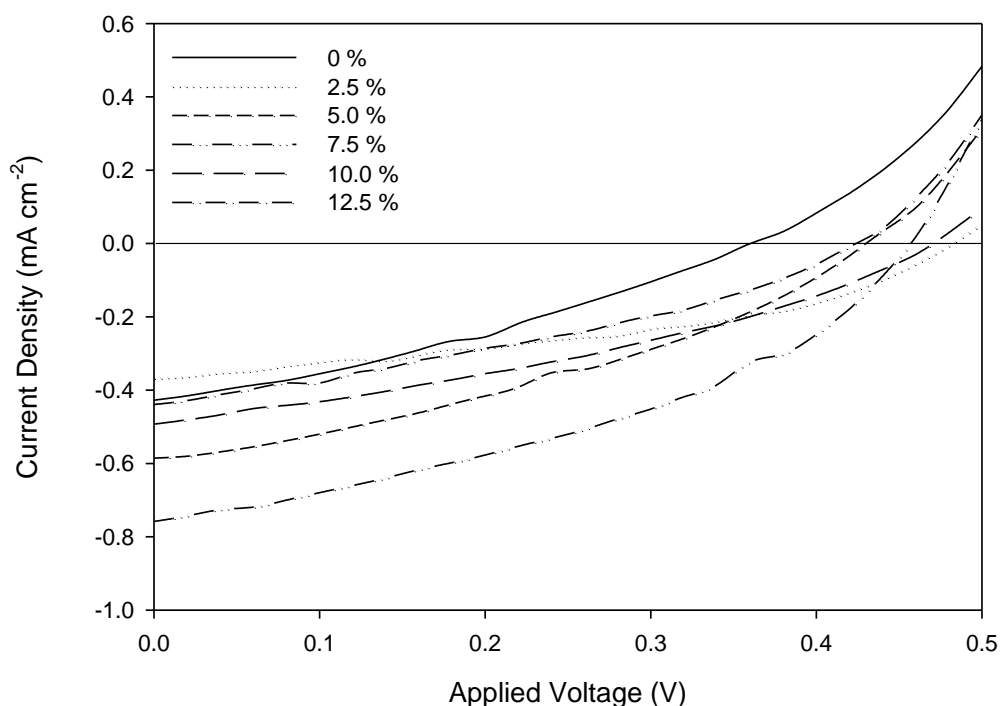

Figure 5. *J-V* curves for untreated and treated TiO_2 photoelectrochemical cells with various concentrations of NH_3

As explained above, the optical absorption represents the excitation of the electrons from the valence band to the conduction band occured in this metal oxide semiconductor materials to explain why the tretaed samples demonstrated much higher efficiency. The absorption windows exist at green region (400-500 nm) for the treated samples increased the opportunity for more electrons migration to

oocur. The lower absorption band gap also contributes to the increasing performance of the treated samples. The efficiency of the treated cells was then decreased as the TiO_2 samples were treated at much higher concentration. Still, the efficiency obtained for the sample fabricated was relatively low compared to other research works due to the lack of absorption capability of the utilized photovoltaic material [23]. The use of the appropriate dye as sensitizer should help to enhance the efficiency of the cell [24]. In overall, nitrogen doping performed on photovoltaic material used in this photoelectrochemical studies enhanced the efficiency of the cell fabricated in this work.

Table 2. Photovoltaic parameters for photoelectrochemical cell TiO_2 treated with various NH_3 concentrations

NH_3 content (%)	J_{sc} (mAcm^{-2})	V_{oc} (V)	η (%)	FF (%)
0	0.43	0.36	0.05	33.2
2.5	0.37	0.48	0.07	40.8
5.0	0.59	0.42	0.09	36.3
7.5	0.76	0.44	0.14	40.6
10.0	0.49	0.46	0.08	35.3
12.5	0.44	0.42	0.06	33.9

4. CONCLUSIONS

We have managed to employ a simple technique in introducing the N species in the TiO_2 nanoparticles by using a spin coating rechnique using various NH_3 concentrations as N source. The TiO_2 was synthesized via LPD method with annealing temperature of 400 ^{o}C. The efficiency measured from the photoelectrochemical cell fabricated with NH_3 treated TiO_2 as photovoltaic material is relatively higher compared with the untreated TiO_2 cell. The highest J_{sc} and power conversion efficiency were 0.76 mA cm^{-2} and 0.14%, respectively obtained from the cell fabricated with 7.5 % NH_3 due to the highest optical absorption the visible region.

References

1. J.A. Leo´n-Ramos, D.K., P. Santiago-Jacinto, Y. Mar-Santiago and M. Trejo-Valdez, *J. Sol. Gel Sci. Technol.*, 57 (2011) 43-50.

2. M. Xing and F. Chen, *Appl. Catal. B: Environ.,* 89 (2009) 563-569.
3. G. John, B.H.F. Rowley, S. Ardo and G.J. Meyer, *J. Phys. Chem. Lett.*, 1 (2010) 3132-3140.
4. Y.K. Chae, S.M., M. Suzuki and J.W. Park, *Chem. Eng. Proc. Tech.*, 2 (2011) 1-4.
5. K.M. Reddy, B.B., M. Jayalakshmi, M.M. Rao and S.V. Manorama, *J. Sol. Chem.*, 178 (2005) 3352-3358.
6. Y.K. Chae and M. Suzuki, *Thin Solid Films*, 517 (2009) 4260-4263.
7. O. Diwald, T. Zubkov, E. G. Goralski, D. Scott, J. Walck and T. Yates, Jr., *J. Phys. Chem. B*, 108 (2004) 6004-6008.
8. J.H. Pan, G.H.R. Zhou and X.S. Zhao, *Chem. Comm.*, 47 (2011) 6942-6944.
9. V.J. Babu, M.K.K., A. S. Nair, T. L. Kheng, S. I. Allakhverdiev and S. Ramakrishna, *Int. J. Hydrogen Energy*, 37 (2002) 8897-8904.
10. N. C. Raut, T.M., K. Panda, B. Sundaravel, S. Dasha and A. K. Tyagi, 2 (2012) 812-815.
11. J. Li, Y.-K. Lai and R.-G. Du, *Surf. Coat. Tech.,* 205 (2010) 557-564.
12. S. In, B. L. Abrams, Y. Hou and I. Chorkendorff, *J. Photochem. Photobiol. A: Chem.*, 222 (2011) 258-262.
13. T. Lindgren, A. Hoel, C.-G. Granqvist, G.R. Torres and S.-E. Lindquist, *Sol. Ener. Mater. Sol. Cells*, 84 (2004) 145-157.
14. Q. Xiang and M.Jaroniec, *Phys. Chem. Chem. Phys.*, 13 (2011) 4853-4861.
15. D. Guti´errez-Tauste, N. Casa˜n-Pastor and J.A. Ayll´on, *J. Photochem. Photobiol. A: Chem.,* 187 (2007) 45-52
16. M.Y.A. Rahman, A.A.Umar, L. Roza and M.M. Salleh, *J. Sol. State Electrochem.*, 12 (2011) 2005-2010.
17. H. Sun, W. Jin and N. Xu, *Sol. Ener. Mater. Sol. Cells*, 92 (2008) 76-83.
18. G. Socrates, Infrared and Raman characteristics group frequencies: Tables and charts*,* (2001) Wiley, New York, 3rd edition.
19. J. Manuel, V.S. Escribano, G. Ramis and G. Busca, *Appl. Catal. B: Environ.*, 13 (1997) 45-58.
20. R. Jin, Z. Wu, H. Wang and T. Gu, *Chemosphere*, 78 (2010) 1160-1166.
21. L.S. Yuan, N.S.H. Razali and H. Nur, *Catal. Comm.*, 20 (2012) 85-88.
22. Y.L. Kuo, F.C. Kung and T.J. Wu, *J. Hazard. Mater.,* 190 (2011) 938-944.
23. W. Guo, Y.S., G.Boschloo, A. Hagfeldt and T. Ma, *Electrochim. Acta*, 56 (2011) 4611-4617.
24. W. Guo, Z. Chen, G. Boschloo, A. Hagfeldt and T. Ma, *J. Photochem. Photobiol. A: Chem.,* 219 (2011) 180-187.